

# Preparation and Characterization of Poly(lactic Acid)-based Composite Reinforced with Oil Palm Empty Fruit Bunch Fiber and Nanosilica

Yin Y. Yee,<sup>a</sup> Yern Chee Ching,<sup>a,\*</sup> Shaifulazuar Rozali,<sup>a</sup> N. Awanis Hashim,<sup>b</sup> and Ramesh Singh<sup>a</sup>

The properties of poly(lactic acid) (PLA) bio-composite films reinforced with oil palm empty fruit bunch (OPEFB) fiber and nanosilica were studied in this work. The composite films were prepared *via* the solvent casting method. The composites were characterized *via* Fourier transform infrared spectroscopy (FTIR), UV-visible spectroscopy, field-emission scanning electron microscopy (FESEM), tensile testing, and X-ray diffraction (XRD). Ultraviolet visible spectroscopy results revealed that the PLA-based composites and neat PLA had similar light transmittances of approximately 89%. The FTIR and FESEM results showed that OPEFB fibers and nanosilica were embedded into the PLA matrix. The tensile strength of the composites with addition of nanosilica increased with an increasing fiber load content. The XRD analysis showed that the addition of organic or inorganic silica reduced the crystallinity of the composites. The water vapor permeability test results indicated that the inorganic silica decreased the diffusion rate of water molecules through the polymer film. The OPEFB-reinforced PLA blend with additional organic silica exhibited a higher thermal stability than the composites reinforced with inorganic silica.

*Keywords:* PLA; OPEFB fiber; Nanosilica; Tensile properties; Reinforcement; Thermal properties

*Contact information:* a: Department of Mechanical Engineering, Faculty of Engineering, University of Malaya, 50603 Kuala Lumpur, Malaysia; b: Department of Chemical Engineering, Faculty of Engineering, University of Malaya, 50603 Kuala Lumpur, Malaysia; \*Corresponding author: chingyc@um.edu.my

## INTRODUCTION

The use of plastic materials has rapidly increased in the last two decades. However, conventional petroleum-based plastic products cannot be degraded or can only be partially degraded in landfills or composting environments (Huda *et al.* 2008). This phenomenon has raised environmental concerns; thus, biodegradable polymers are currently being studied because they are renewable and possess favorable properties (Bajpai *et al.* 2012). The synthesis of polymers through the use of monomers from natural resources has provided a new direction in the development of biodegradable polymers from renewable resources. Current trends in biodegradable polymers reveal new expansion in strategies and engineering to attain polymeric materials with high attention both in the industrial and academic areas (Bajpai *et al.* 2012). According to Valdés *et al.* (2014), starch, poly(lactic acid) (PLA), and polyhydroxyalkanoates (PHA) are the most widely studied biopolymers. Given that PLA is made from agricultural products, it is biodegradable, biocompatible, and has high strength and modulus (Garlotta 2001). The polymerization of lactic acid produces lactide, a cyclic dimer, which can be obtained through the fermenting of corn, sugar cane, and sugar beet (Lunt 1998). However,

biodegradable polymers obtained from renewable resources also have several disadvantages, including their hydrophilic nature, rapid degradation rate, and poor mechanical properties, especially in wet environments (Yu *et al.* 2006).

PLA composites reinforced with natural fibers are 100% bio-based materials with favorable mechanical properties compared to commercial petroleum-based products. In general, the properties of polymers can be modified using fillers and fibers. Previous studies involved the addition of various natural fibers to different polymer matrices. Natural fibers are biodegradable because they are obtained from plants, and they are non-abrasive as well. Natural fibers are abundant, low-cost, and have a low density. Thus, they can be used as alternatives to synthetic fibers in environmental applications (Du *et al.* 2014). The development of natural fiber composites has attracted research interest for the last few years because the fibers can replace conventional reinforcement materials, in terms of weight reduction (Kumar and Sekaran 2014). Natural fiber-reinforced polymer composites exhibit high mechanical properties and have specific advantages during processing (Kumar and Sekaran 2014). Poly(lactic acid) (PLA) reinforced with kenaf (Huda *et al.* 2008), bamboo (Kang and Kim 2011), banana (Shih and Huang 2011), ramie (Yu *et al.* 2010), oil palm (Rayung *et al.* 2014), and other natural fibers have been studied. However, the use of these natural fibers have several drawbacks, such as incompatibility with hydrophobic polymer matrices, poor resistance to moisture, low degradation temperatures, and a higher tendency towards agglomeration during processing (Rayung *et al.* 2014; Tan *et al.* 2015). Therefore, fillers such as silica, aluminium, and zinc oxide have been further introduced into polymer composites to enhance their performance.

Recently, nano-sized fillers have been formulated and incorporated with biopolymers to improve their properties, such as stiffness, permeability, crystallinity, and thermal stability (Bordes *et al.* 2009; Khoon *et al.* 2015). These reinforced biopolymers are commonly used in the production and processing of polymeric materials. The mechanical properties of these polymeric materials can be significantly improved by adding a small amount of filler. Nanosilica is a commonly used filler in polymer composites because of its contribution to thermal stability and mechanical properties (Yan *et al.* 2007b; Battagazzore *et al.* 2014). Silica can be obtained from rice husk, groundnut shell, bamboo leaves, and sugarcane bagasse (Vaibhav *et al.* 2015). Extraction of silica from bamboo leaves is a new trend in the current research field. A large amount of bamboo leaves are treated as waste and disposed of at landfill sites. Battagazzore *et al.* (2014) performed the reinforcement of silica extracted from rice husk and formulated it into the PLA matrix. It was found that the extracted silica from the rice husks enhanced the barrier properties and storage modulus of the PLA composites, as well as Young's modulus.

There are several promising markets for biodegradable polymers. Incorporation of functional fillers in the PLA matrix could improve the physical properties, as well as the surface characteristics of the matrix that can be applied for various applications such as barriers for sanitary products and diapers, disposable cups and plates (Oksman *et al.* 2003), packaging industry, electronic industry, biomedical, automobiles, infrastructure, and furniture (Bajpai *et al.* 2012). In this study, a biopolymer composite based on PLA was reinforced with oil palm empty fruit bunch (OPEFB) fiber and silica. Two types of silica were used in this study: commercial inorganic silica and organic silica extracted from bamboo leaves. The effect of OPEFB fiber load (0.5, 1.0, and 1.5 wt.%) reinforced

with the PLA matrix were investigated. The properties of the OPEFB-reinforced PLA composites were further reinforced with the addition of nanosilica.

The aim for this work was to study the reinforcement materials on the mechanical, thermal, optical, and water barrier properties of PLA-based biopolymer composites. The physical and chemical properties of the composites were performed through Fourier transform infrared spectroscopy (FTIR) and X-ray diffraction (XRD). Field-emission scanning electron microscopy (FESEM) was conducted to study the structural detail of the composites. Water vapor permeability and optical properties of the composites were studied to compare the effects of organic *versus* inorganic nanosilica on the water barrier properties and transparency of the PLA/OPEFB composite film.

## EXPERIMENTAL

### Materials

Poly(lactic acid) (3052D Ingeo™, specific gravity 1.24, melt flow index (MFI) 14 g /10 min at 210 °C 216 kg, relative viscosity 3.3) was purchased from NatureWorks LLC, USA. The OPEFB fibers were collected from FELCRA Nasiruddin Oil Palm Mill, Perak, Malaysia. Bamboo leaves were collected from a garden in the University of Malaya's garden (Kuala Lumpur, Malaysia). Inorganic nanosilica (Aerosil 200) was purchased from Degussa (Germany). Nitric acid (69%) and chloroform were purchased from Fisher Scientific (M) Sdn. Bhd. Both of the chemicals were of AR grade and were used without further purification.

### Methods

#### *Extraction of nanosilica from bamboo leaves*

Approximately 500 g of bamboo leaves was first acid leached with 1.5 M of nitric acid, stirred for 18 h, and then continuously washed with distilled water until a pH of 7 was reached. The leaves were left to air dry for one day and then burnt in a furnace at 600 °C with 10 h of ramping and 10 h of isothermal heat. The bamboo silica residues (nanosize), which are referred to as organic silica in this study, were stored in desiccators.

#### *Preparation of composite films*

The OPEFB fibers were pulverized using a sieve shaker. The PLA and PLA-based composite films were prepared *via* the solvent-casting method. Approximately 7 g of PLA resin was dissolved in 100 mL of chloroform and was added to different filler contents (0.5, 1.0, and 1.5 wt.% OPEFB fibers; 1.0 wt.% for both organic and inorganic silica) to form samples with various compositions. The mixture was then vigorously stirred using a magnetic stirrer for at least 5 h at room temperature.

The solution was then poured onto a glass plate (20-cm diameter) and allowed to dry for 24 h at room temperature. All PLA films were further oven-dried at 60 °C for 2 d to ensure that all of the remaining chloroform solvents were removed. This step was performed to prevent the chloroform solvent from acting as a plasticizer (Rhim *et al.* 2006). The thickness of the sample films prepared was 0.2 mm. All film samples were preconditioned at 25 °C and 50% relative humidity in a temperature humidity chamber for at least 48 h before characterization. The prepared PLA and PLA-based composites are listed in Table 1.

**Table 1.** Nomenclature and Compositions of PLA and PLA-based Composites

	Sample	PLA (wt%)	EFB (wt%)	OrSiO <sub>2</sub> (wt%)	InSiO <sub>2</sub> (wt%)
1	PLA	100	-	-	-
2	PLA/OrSiO <sub>2</sub>	99	-	1	-
3	PLA/InSiO <sub>2</sub>	99	-	-	1
4	PLA/EFB-0.5	99.5	0.5	-	-
5	PLA/EFB-0.5/OrSiO <sub>2</sub>	98.5	0.5	1	-
6	PLA/EFB-0.5/InSiO <sub>2</sub>	98.5	0.5	-	1
7	PLA/EFB-1	99	1	-	-
8	PLA/EFB-1/OrSiO <sub>2</sub>	98	1	1	-
9	PLA/EFB-1/InSiO <sub>2</sub>	98	1	-	1
10	PLA/EFB-1.5	98.5	1.5	-	-
11	PLA/EFB-1.5/OrSiO <sub>2</sub>	97.5	1.5	1	-
12	PLA/EFB-1.5/OrSiO <sub>2</sub>	97.5	1.5	-	1

### Characterization

The chemical structures of PLA, OPEFB, and nanosilica were evaluated *via* FTIR Spectrum 400 (Perkin Elmer, USA) using diamond attenuated total reflectance (ATR) techniques. The ATR spectra were obtained in a scan range between 4000 to 450 cm<sup>-1</sup>, a scan rate of 32 unit scans, and a resolution of 4 cm<sup>-1</sup>. The transparency of the films was determined by measuring the percent transmittance at 660 nm using a UV/VIS spectrophotometer (Model Cary 50 UV-VIS, Varian Inc., USA).

The surface morphologies of the PLA composites were observed and analyzed *via* FESEM (model JEOL JSM-7600F, Japan) at room temperature. The samples were coated with a thin film of platinum to avoid a charging effect.

Tensile tests were performed using an Autograph AGS-X Universal Tester (Shimadzu, Japan) according to the ASTM D882 standard. Initial grip separation was set at 50 mm, and a cross-head speed at 50 mm/min was employed. Five specimens were tested for each combination of composite, and the tensile properties, such as tensile strength, Young's modulus, and elongation at break, were recorded.

The structural changes of the PLA composites films were characterized using a Rigaku (Japan) X-ray diffractometer (operated at 40 kV and 40 mA) with CuK $\alpha$  radiation, and at a wavelength of 1.5460 Å. The intensity data were collected over a 2 $\theta$  range from 10° to 30°, and at a scan rate of 0.05°/s. The degree of crystallinity,  $\chi_c$  was computed using Eq. 1,

$$\chi_c = A_c / A_c + A_a \quad (1)$$

where  $A_c$  and  $A_a$  are the crystallized and amorphous areas on the x-ray diffractogram, respectively.

Water vapor permeability tests were conducted using a water vapor transmission rate tester (PERME-W3/030, Labthink, China). Each specimen was prepared in a circular shape (33 cm<sup>2</sup>), and the test gap was set at 120 min. The specimen underwent 2 h of pre-equilibrium, and the stability condition was set at 10%. The temperature inside the chamber was controlled at 38 °C and 90% relative humidity.

Thermogravimetric analysis (TGA) tests were performed using a Mettler Toledo TGA/SDTA851 thermogravimeter (Mettler Toledo Coro, Switzerland). Each sample (8 to 10 g) was heated from 30 to 500 °C at 10 °C min<sup>-1</sup> with an air flow.

## RESULTS AND DISCUSSION

### FTIR Spectra

Figure 1 shows a comparison of the chemical structure of inorganic silica *versus* inorganic silica extracted from bamboo leaves. Commercial inorganic silica has peaks at 1071 and 806  $\text{cm}^{-1}$ , which can be assigned to the Si-O-Si stretching and bending vibrations (Battezzore *et al.* 2014). On the other hand, organic silica extracted from bamboo leaves also contained the same functional group at wavenumbers 1051 and 796  $\text{cm}^{-1}$ . The broad band between 3700 and 2800  $\text{cm}^{-1}$  (centered at 3384  $\text{cm}^{-1}$ ) correspond to OH stretching, whereas the peak at 976  $\text{cm}^{-1}$  was assigned to the formation of the Si-OH bond (Wu and Liao 2008). The peak at 1636  $\text{cm}^{-1}$  was attributed to the aromatic skeletal vibrations of lignin.

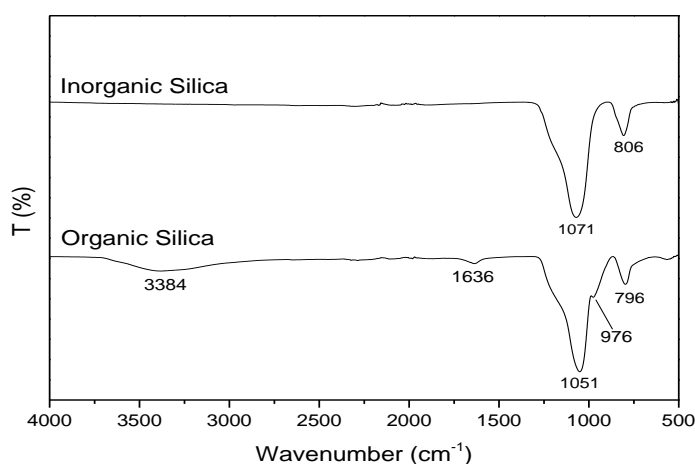


**Fig. 1.** Comparison of FTIR spectra of organic silica extracted from bamboo leaves and commercial inorganic silica

The IR spectra of neat PLA and PLA-based composite films with various compositions of OPEFB fibers are shown in Fig. 2. The main absorbances of the samples appeared at regions of low wavenumber, specifically from 500  $\text{cm}^{-1}$  to 1800  $\text{cm}^{-1}$ . However, characteristic peaks for PLA were observed at the 2800  $\text{cm}^{-1}$  to 3000  $\text{cm}^{-1}$  region (Wu and Liao 2008). The spectrum of OPEFB was similar to that in the work of Siyamak *et al.* (2012), where main peaks are located almost at the same wavenumbers (3340, 2900, 1729, and 1604  $\text{cm}^{-1}$ ). These peaks corresponded to the OH bending of cellulose, the C-H stretching in aromatic methoxyl groups of cellulose, and hemicellulose, C=O stretching of either acetyl or uronic ester groups of hemicelluloses, and C=C aromatic skeletal vibrations of lignin, respectively (Ching and Ng 2014). In this study, the interaction between the OPEFB filler and the PLA matrix was mainly physical because no significant peaks or obvious shifting were observed compared to the neat PLA spectrum (Qu *et al.* 2010). However, several small peaks were observed at the wavenumbers of 1210, 1293, and 1755  $\text{cm}^{-1}$  as shown in Fig. 2. Both peaks at 1210 and 1293  $\text{cm}^{-1}$  were attributed to the OH bending vibrations of cellulose (Siyamak *et al.* 2012). The peak at 1755  $\text{cm}^{-1}$  was attributed to the stretching of C=O of lignin (Ng *et al.* 2014; Ching *et al.* 2015). The significant peaks of OPEFB fibers were not observed in the fiber-reinforced PLA composites because they may have been covered by other strong peaks of PLA, given that the amount of fibers was minimal compared to that of the PLA

polymer matrix. The presence of these peaks at 1210, 1293, and 1755  $\text{cm}^{-1}$  indicated that the fibers had been introduced into the polymer matrix.

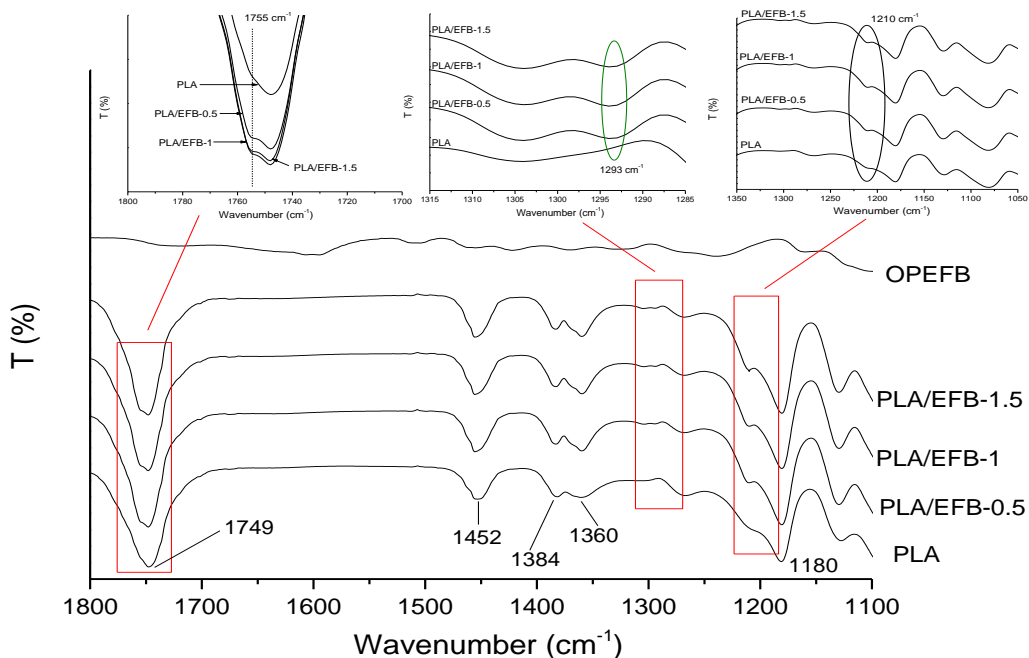


**Fig. 2.** The FTIR spectra of neat PLA and OPEFB-reinforced PLA composite films

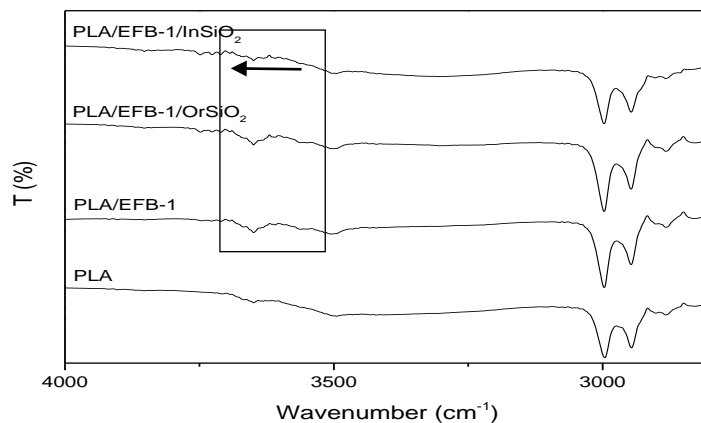


**Fig. 3.** The FTIR spectra of PLA/EFB composite film reinforced with nanosilica (inorganic and organic)

Organic nanosilica extracted from bamboo leaves was used to reinforce the PLA/EFB composites. Figure 3 shows the spectra of 1.0 wt.% fiber-reinforced PLA with 1.0 wt.% organic or inorganic silica. There was a shift of the broad band ( $\sim 3500$  to  $3800$   $\text{cm}^{-1}$ ) to the left corresponds to the OH stretching (Wu and Liao 2008). This phenomenon occurred because of the existence of hetero-associated hydrogen bonds that formed between the carboxylic acid groups of PLA and the silica bonded group (Wu and Liao 2008). Hydrogen bonding was the only interfacial force that facilitated the interconnection between the PLA matrix and the nanosilica reinforcement network.

### Film Optical Property

Figure 4 shows the transmittance percentage of PLA composite films at wavelengths of 400 to 700 nm. The optical transmission of PLA composite films decreased after addition of reinforcement materials. The neat PLA film had the highest transmittance among all the PLA-based films at the visible region, which was 79.8%, followed by PLA/EFB-1 at 78.3%. On the other hand, 1.0 wt.% of inorganic nanosilica-reinforced composite film exhibited a similar optical transmittance to the PLA composites, with 1.0 wt.% fiber filler, which was 77.8%. However, the light transmission of PLA/EFB-1.5/InSiO<sub>2</sub> composite had been reduced to 75% with the increase of fibers content from 1.0 wt.% to 1.5 wt.%. Composites containing 1.0 wt.% of organic nanosilica showed low light transmittances, and the values were 75.4% and 72.7% for 1.0 wt.% and 1.5 wt.% fiber load, respectively.

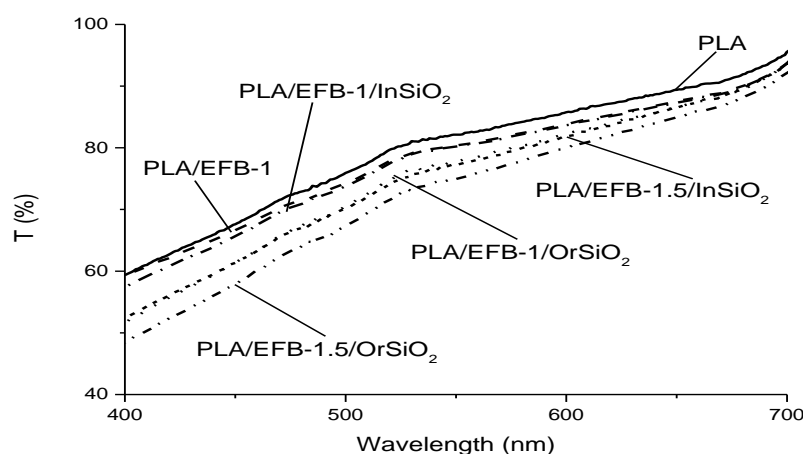


**Fig. 4.** Visible light transmission of PLA/EFB composite films reinforced with nanosilica

In comparison with organic silica, inorganic silica allowed more visible light to pass through. According to Zeng *et al.* (2005), when a reinforced material with a size of approximately 1.0 nm is thoroughly dispersed in the polymer matrix, the transmittance percentage is similar to that of the original polymer. Nano-sized materials will not hinder the passage of light because their sizes are less than the wavelength of visible light. The low light transmission of composites with organic nanosilica as the filler indicates that the organic nanosilica was not evenly distributed in the polymer matrix. This result indicates that the organic silica had agglomerated. Moreover, cold crystallization might have occurred during solvent casting, and the silica may have functioned as a nucleating agent (Rhim *et al.* 2009).

### FESEM

Morphological analysis was performed to evaluate the OPEFB fiber and silica dispersion throughout the polymer matrix. Figure 5a illustrates that the addition of 0.5 wt.% OPEFB fibers into the PLA polymer matrix resulted in a homogeneous distribution. However, a small amount of agglomerates were observed in PLA/EFB-1 (Fig. 5b), where the segregation between the reinforcement material and the polymer matrix was low. This result shows that the fibers cannot be distributed well in the matrix when they are added at high amounts because of the hydrophilic properties of the fibers and their tendency to agglomerate as a result of hydrogen bonding.

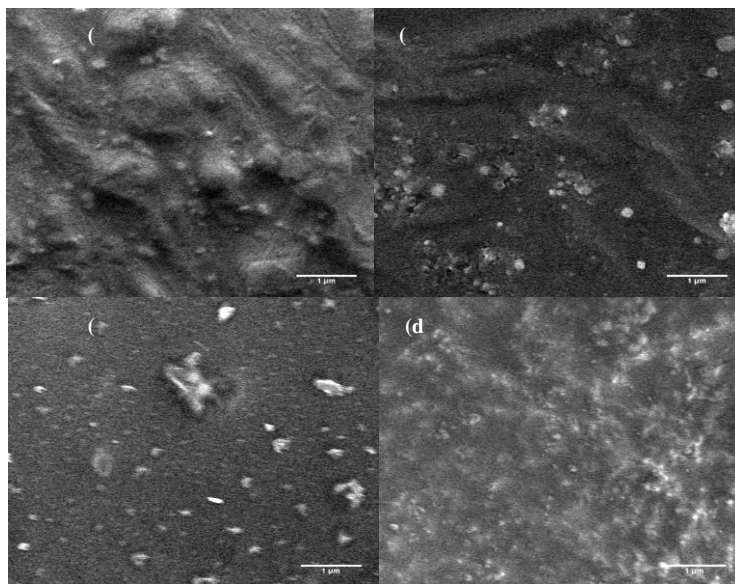


**Fig. 5.** The FESEM images of PLA-based composite films reinforced with (a) 0.5 wt.% fiber, (b) 1.0 wt.% fiber, (c) 1.0 wt.% fiber + 1.0 wt.% organic silica, and (d) 1.0 wt.% fiber + 1.0 wt.% inorganic silica

The same observation was found in PLA composite films with 1.0 wt.% of OPEFB fibers and 1.0 wt.% of organic silica. The fibers and silica were embedded in the polymer matrix (Fig. 5c). However, silica extracted from bamboo leaves presented hydrophilic characteristics, even though its main components were the same as those of common plant leaves, namely, cellulose, hemicelluloses, and lignin (from FTIR). When added to the PLA matrix, the fibers and organic silica tended to agglomerate easily because of the strong hydrogen bond formation between these two organic components. Given the high surface energy and surface polarity differences between the reinforcement and the polymer matrix, agglomeration can be minimized by vigorously agitating the mixture (Yan *et al.* 2007b). For PLA-based composites with OPEFB fibers and inorganic silica, the reinforcement was uniformly dispersed into the PLA matrix with slight agglomeration. This result indicates that the presence of inorganic silica assists in surface adhesion between the filler and the matrix (Fig. 5d). To further enhance the adhesion between the fillers and the matrix, the fibers must be subjected to a surface treatment, such as an alkaline or silane treatment, to improve the properties of the composite (Yu *et al.* 2010; Ali *et al.* 2014; Ching and Ng 2014).

### Tensile Properties

The effects of adding various compositions of OPEFB fibers (0.5, 1.0, and 1.5 wt.%), organic silica, and inorganic silica on the tensile properties of PLA-based composites are shown in Figs. 6 to 8. Theoretically, the tensile strength of the reinforcement polymer composite increases with increasing filler content (Azman *et al.* 2013; Tahan *et al.* 2013). A well-developed nanocomposite with uniformly dispersed reinforcement particles produces strong interfacial adhesion between the fillers and the host polymer, thereby resulting in a large increase in mechanical strength, compared to the neat polymer alone (Bajpai *et al.* 2012). Yu *et al.* (2010) also proposed that the increase in tensile strength and stiffness with the addition of the filler to the polymer

matrix resulted in improved surface compatibility and good stress transfer between the reinforcement and the polymer matrix. However, the results obtained in the present study were not the same as those reported in the literature. Figure 6 indicates that neat PLA showed the highest tensile strength (*i.e.*, 48 MPa) among all the composites. The tensile strength of the neat PLA decreased from 48 MPa to 29 MPa after 1.5 wt.% OPEFB fiber was introduced to the PLA matrix. The tensile strength of the PLA/OPEFB decreased with increasing of OPEFB fiber loads. This trend can be explained by the hydrophilic nature of lignin in the OPEFB fibers and is therefore concluded to be incompatible with the PLA matrix. The nonuniform stress transfer caused by the agglomeration of fibers in the matrix also resulted in composite failure (Huda *et al.* 2008; Nurfatimah *et al.* 2014). Fiber-fiber interactions increase with increasing fiber content. This interaction, therefore, led to the formation of voids, which can be sites of crack propagation in the composite, resulting in a decay in tensile strength (Kang and Kim 2011; Siyamak *et al.* 2012).

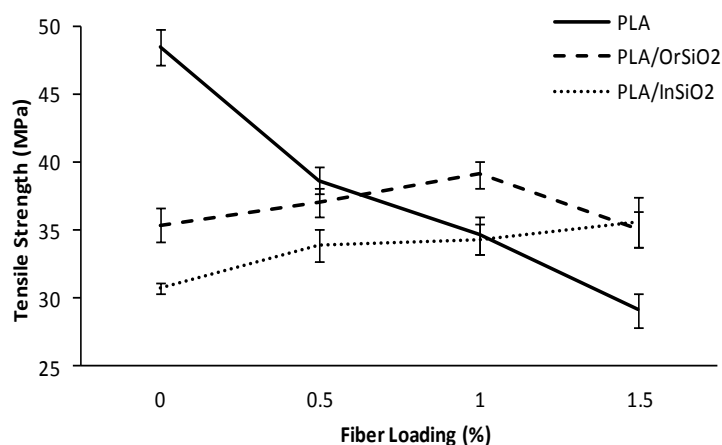


**Fig. 6.** Tensile strength profiles of neat PLA and PLA reinforced with EFB fiber and nanosilica

In the case of PLA reinforced with organic silica and inorganic silica, increasing the fiber loading enhanced the tensile strength of the composites. The tensile strength of the organic silica-reinforced PLA composite was 35 MPa, whereas the composite with 0.5 wt.% fiber and 1.0 wt.% organic silica reached 37 MPa. The PLA/OrSiO<sub>2</sub> composite with 1.0 wt.% OPEFB fibers exhibited the highest tensile strength of 39 MPa. This result indicates that the stress applied on the PLA matrix was successfully transferred to the reinforced materials. However, the tensile strength for the PLA/OrSiO<sub>2</sub> composite with further addition of OPEFB to 1.5 wt.% decreased significantly. This might be due to the agglomeration between fiber and fiber or fiber and organic silica. This agglomeration was caused by the hydrophilic characteristics of both the fiber and organic silica (Yang *et al.* 2007). Hydrophilic nature of the organic silica and fiber could not form a good interaction with hydrophobic polymer matrix (Saba *et al.* 2014). Thus each particle site would serve as the centre of stress concentration, thereby reducing the ability to transfer stress efficiently. For PLA/OPEFB composite reinforced with inorganic silica, the tensile strength increased with increasing fiber loading. Similar observations had been reported by Shi *et al.* (2010) for poly(lactic acid)/bamboo fiber/talc composites and Mustapa *et al.* (2013) for poly(lactic acid)/hemp fiber reinforced with nanosilica.

A similar trend was observed for the effect of fillers to the tensile modulus properties of PLA composites. The addition of fibers into PLA caused a significant decrease in the tensile modulus of the composites, as shown in Fig. 7. The Young's

modulus increased with increasing fiber loading in both the PLA/OrSiO<sub>2</sub> and PLA/InSiO<sub>2</sub> composites because the fibers functioned as fillers to absorb the stress transferred from the PLA matrix. In other words, the addition of nanosilica increased the interfacial adhesion between the fibers and the PLA matrix. In this study, the PLA composite reinforced with 1.0 wt.% fiber and 1.0 wt.% of organic silica had the highest Young's modulus.

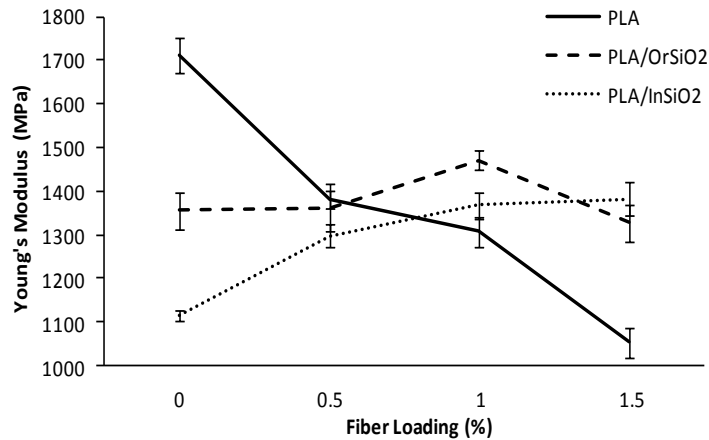


**Fig. 7.** Young's modulus profiles of neat PLA and PLA reinforced with EFB fiber and nanosilica

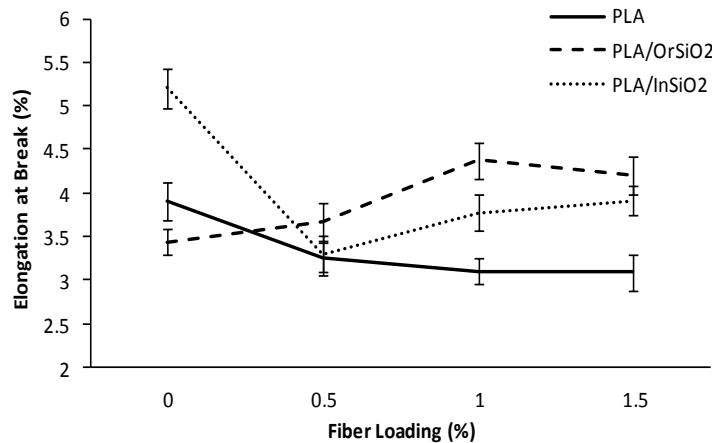


**Fig. 8.** Elongation at break (%) profiles of neat PLA and PLA reinforced with EFB fiber and nanosilica

Figure 8 shows the elongation at break of the PLA-based composites. The elongation at break was affected by the volume fraction of the added reinforcements and their dispersion in the composite (Fortunati *et al.* 2012). The PLA and PLA-based composites were both characteristically brittle materials, with all specimens breaking at a short period of time after yielding (Yan *et al.* 2007b). Generally, the elongation at break decreases when reinforcement materials are added into the composite because these reinforcements cause stress concentrations (Pettersson and Oksman 2006). In this study, the elongation of PLA decreased with increasing of OPEFB fiber. However, PLA reinforced with inorganic silica exhibited ductile behavior, which was attributed to an elastic region at low displacements followed by a nonlinear behavior prior to the yield point and plastically deformed at a constant load before fracturing. Therefore, PLA

reinforced with 1.0 wt.% inorganic silica showed the highest percentage of elongation at break compared with other composites. This phenomenon might have occurred because of the hydrophobic nature of inorganic silica (Shi *et al.* 2014). Thus, it forms a stable hindrance layer between particles and inhibits the formation of aggregates, thereby improving the degree of dispersion of the high percentage of fiber in the PLA matrix. Figure 8 shows that the elongation of PLA/OrSiO<sub>2</sub> composite increased with the increase of OPEFB fiber. This result indicates that the organic silica assisted in good dispersion of OPEFB fiber within the PLA matrix.

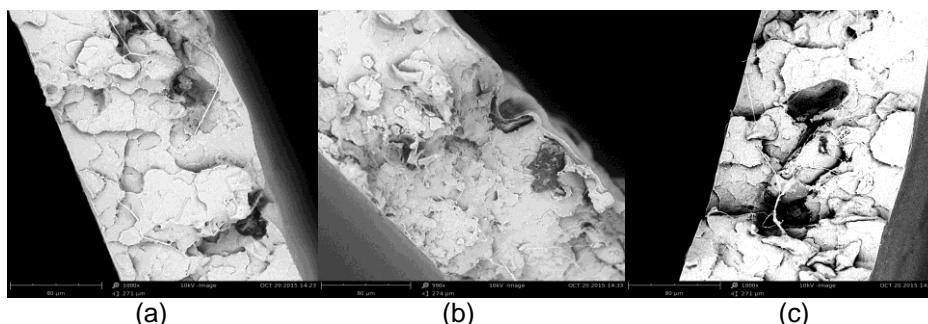


**Fig. 9.** The SEM images of fracture surface of PLA-based composite films (a) PLA/EFB-1 (b) PLA/EFB-1/OrSiO<sub>2</sub> and (c) PLA/EFB-1/InSiO<sub>2</sub>

Figure 9 shows the effect of silica filler to fracture surface of the PLA/EFB-1 composites. It can be seen that there were holes extending into the polymer matrix, which indicates that the fibers had been pulled out from the polymer surface for composite PLA/EFB-1 (Fig. 9(a)) and PLA/EFB-1/InSiO<sub>2</sub> (Fig. 9(c)). This result reveals that there was poor adhesion between fibers and PLA matrix since fiber did not show a clear break together with polymer matrix. However, fiber in PLA/EFB-1/OrSiO<sub>2</sub> composite as shown in Fig. 9(b) fractured together with PLA matrix when undergoing the tensile test. The stress load was absorbed by the fiber. Therefore, the composite had higher tensile properties compared to the neat PLA and PLA/EFB-1/InSiO<sub>2</sub> composites.

## XRD

The XRD patterns of PLA and PLA-based composite films at 10° to 30° (2 $\theta$ ) are shown in Fig. 10. The crystallinity of composites was discussed in respect of the peak areas obtained through integration and degree of crystallinity. As shown in Fig. 10, several peaks indicate that the neat PLA and PLA-based composites are semicrystalline materials. The strongest diffraction peak for all of the samples was observed at approximately 2 $\theta$  = 16°, which corresponds to the (200, 110) reflection of  $\alpha$ -form crystals. Other intense peaks at 2 $\theta$  = 19° and 22° were ascribed to the crystal structure of PLA (Chen *et al.* 2012). The XRD patterns of neat PLA and PLA with 1.0 wt.% of EFB exhibited no significant differences from each other, with the degree of crystallinity of 25% and 24.2%, respectively. This result indicates that adding a small amount of fiber does not affect the crystallinity of the composite. However, with the addition of 1.0 wt.% of silica filler into PLA/EFB composites, there was a significant drop on the crystalline peak intensity of PLA. The crystallinity of PLA/EFB-1/OrSiO<sub>2</sub> has decreased to 15.5%, which is slightly higher compared to PLA/EFB-1/InSiO<sub>2</sub> with 11.1%. This result implies that the addition of organic or inorganic silica has further decreased the crystallinity of composite. Wang *et al.* (2015) also reported the same trend in their study on polyvinylamine (PVAm)/silica composite that the addition of inorganic silica will

decrease the crystallinity of polymer composite. According to Yan *et al.* (2007a), the decrease of peak intensity was probably due to the poor crystallized macromolecules. Besides, the small and metastable crystals might be strictly confined by the rigid silica network thus resulted in the decrease of crystallinity of the composite.

Figure 10 also illustrates that the crystallinity was further reduced when the EFB fiber was increased from 1 wt.% to 1.5 wt.% for both the organic and inorganic silica reinforced PLA/EFB composites. In summary, the relative crystallinity of the reinforced PLA-based composites decreased with increasing amounts of reinforced materials.

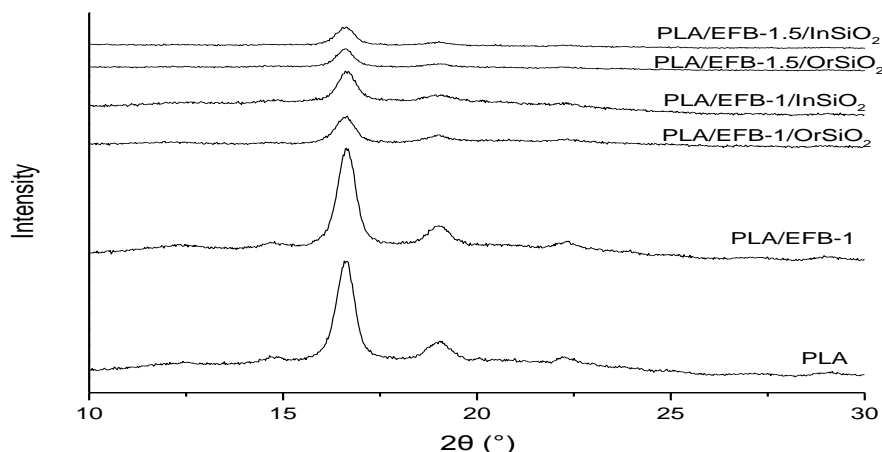


**Fig. 10.** X-rays diffraction of PLA and PLA reinforced with EFB fiber and nanosilica composite film

### Water Vapor Permeability (WVP)

Water vapor permeability is an important parameter in the packaging industry. The WVP values of PLA and PLA-based composite films are summarized in Table 2. The WVP of the composites was affected by the presence of fibers and silica. The WVP values of composite films with fibers and organic silica increased; however, only those of composite films reinforced with inorganic silica decreased. This phenomenon was attributed to the hydrophobicity of inorganic silica, which contributes to the homogeneous dispersion of the reinforcement materials in the PLA matrix to form a good adhesion layer between the filler and the matrix.

**Table 2.** Water Vapor Permeability of PLA and PLA-based Composites

Films	WVP ( $\times 10^{-15}$ g m/m <sup>2</sup> s Pa)
PLA	5.90
PLA/EFB-1	8.29
PLA/EFB-1/ OrSiO <sub>2</sub>	8.79
PLA/EFB-1/InSiO <sub>2</sub>	5.64
PLA/EFB-1.5/OrSiO <sub>2</sub>	9.11

The well-dispersed inorganic silica increases the effective distance or tortuous path of water vapor molecules when they diffuse through the composite film (Ray and Okamoto 2003). Thus, WVP increases with an increasing fiber load. Fibers and organic

silica are hydrophilic; thus, they tend to form agglomerates (Yang *et al.* 2007). The weak interaction between the reinforcements and the matrix form a shorter path for the water vapor molecules to pass through the composite films (Petersson and Oksman 2006).

## TGA

The thermal stability of neat PLA and PLA-based composites was investigated and compared in terms of weight loss as a function of temperature using thermogravimetric analysis (TGA). Thermal degradation of neat PLA occurred in a single step, in which the maximum weight loss was observed at 367 °C. As shown in Fig. 11, there were two main degradation regions for the PLA-based composites. The first one occurred at the range of 80 to 150 °C, which was the evaporation of moisture that occurred during the drying process of the specimens. The second degradation was observed at 270 to 380 °C, which was attributed to the thermal degradation of cellulosic substances of cellulose, hemicelluloses, lignin, and the depolymerization of PLA (Kim *et al.* 2008).

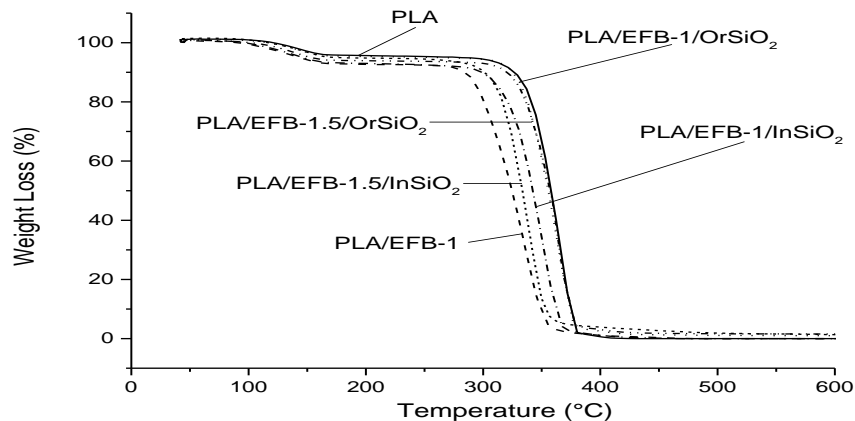


**Fig. 11.** The TG curves of neat PLA and PLA-based composites in air

As shown in Fig. 11, PLA reinforced with 1.0 wt.% OPEFB fiber exhibited the lowest degradation temperature of 339 °C. The addition of natural fibers decreased the thermal stability of neat PLA. This was caused by a portion of the PLA matrix that had been replaced by natural fibers, which are thermally low stable materials (Ching *et al.* 2013; Yong *et al.* 2015). Previous studies also obtained the same results, where the addition of natural fibers reduced the thermal stability of the polymer matrix (Ng *et al.* 2014; Nurfatimah *et al.* 2015). However, with the addition of silica, the degradation temperature of the polymer shifted to higher temperatures. These result were expected because silica is thermally stable at temperature up to 800 °C (Battezzore *et al.* 2014). Silica was introduced to enhance the performance of the composites by acting as a superior insulator and mass transport barrier against the volatile products generated during decomposition (Yan *et al.* 2007a). Zhang *et al.* (2008) found that the addition of silica improved the degradation temperature of PLA composites. Similarly, Yan *et al.* (2007b) also observed that the thermal motion of the polymer was restricted by the silica network. In Fig. 11, PLA composites reinforced with 1.0 wt.% of organic silica were more thermally stable than composites reinforced with 1.0 wt.% of inorganic silica. Both composites reinforced with organic silica (1.0 wt.% and 1.5 wt.% of fibers load) had

almost the same degradation temperature compared to neat PLA, which were 364 and 365 °C, respectively. However, PLA/InSiO<sub>2</sub> composite containing 1.5 wt.% OPEFB fiber showed lower degradation temperature of 337 °C compared to PLA/InSiO<sub>2</sub> composite reinforced with 1.0 wt.% OPEFB fiber.

## CONCLUSIONS

PLA-based composites were prepared by a solvent casting method with OPEFB fibers, organic silica, and inorganic silica as fillers. The properties of composites were investigated and compared.

1. The optical transmission of PLA composite films decreased with increasing filler content.
2. The mechanical properties of the PLA/EFB composites were improved with the introduction of silica fillers. The PLA/EFB composites with organic silica exhibited better mechanical properties than the composites reinforced with inorganic silica.
3. The WVP values of the composite increased with increasing fiber content. Inorganic silica reduced the WVP property because of its hydrophobicity and even distribution in the matrix.
4. Both the addition of organic and inorganic silica had reduced the crystallinity of the PLA matrix.
5. Organic silica increased the thermal stability of fiber-reinforced PLA compared to composites reinforced with inorganic silica by restricting the thermal motion of polymer.

## ACKNOWLEDGMENTS

The authors would like to acknowledge financial support from the High Impact Research MoE Grant UM.C/625/1/HIR/MoE/52 from the Ministry of Education Malaysia, RU022A-2014, RP011A-13AET, FP030-2013A, and RG031-15AET for the success of this project.

## REFERENCES CITED

- Ali, M. E., Yong, C. K., Ching, Y. C., Chuah, C. H., and Liou, N. S. (2014). "Effect of single and double stage chemically treated kenaf fibers on mechanical properties of polyvinyl alcohol film," *BioResources* 10(1), 822-838. DOI: 10.15376/biores.10.1.822-838
- ASTM D882. (2012). "Standard test methods for tensile properties of thin plastic sheeting," *ASTM International*, West Conshohocken, PA. DOI: 10.1520/D0882-12
- Azman, H., Mat, U. W., and Ching, Y. C. (2003). "Mechanical and morphological properties of PP/NR/LLDPE ternary blend. Effect of HVA-2," *Polymer Testing* 22, 281-290.

- Battegazzore, D., Bocchini, S., Alongi, J., and Frache, A. (2014). "Rice husk as bio-source of silica: Preparation and characterization of PLA–silica bio-composites," *RSC Advances* 4(97), 54703-54712. DOI: 10.1039/C4RA05991C
- Bajpai, P. K., Singh, I., and Madaan, J. (2012). "Development and characterization of PLA-based green composites: A review," *Journal of Thermoplastic Composite Materials* 27(1), 52-81. DOI: 10.1177/0892705712439571
- Bordes, P., Pollet, E., and Avérous, L. (2009). "Nano-biocomposites: Biodegradable polyester/nanoclay systems," *Progress in Polymer Science* 34(2), 125-155. DOI: 10.1016/j.progpolymsci.2008.10.002
- Chen, B.-K., Shih, C.-C., and Chen, A. F. (2012). "Ductile PLA nanocomposites with improved thermal stability," *Composites Part A: Applied Science & Manufacturing* 43(12), 2289-2295. DOI: 10.1016/j.compositesa.2012.08.007
- Ching, Y. C., and Ng, T. S. (2014). "Effect of preparation conditions on cellulose from oil palm empty fruit bunch fiber," *BioResources* 9(4), 6373-6385. DOI: 10.15376/biores.9.4.6373-638.
- Ching, Y. C., Rahman, A., Ching, K. Y., Sukiman, N. L., and Cheng, H. C. (2015). "Preparation and characterization of polyvinyl alcohol-based composite reinforced with nanocellulose and nanosilica," *BioResources* 10(2), 3364-3377. DOI: 10.15376/biores.10.2.3364-3377
- Ching Y. C., Goh, K. Y., Luqman, C. A., and Kalyani, N. (2013). "Effect of nanosilica and titania on thermal stability of polypropylene/oil palm empty fruit fibre composite," *J. Biobased Materials and Bioenergy* 7, 169-174.
- Du, Y., Yan, N., and Kortschot, M. T. (2014). "A simplified fabrication process for biofiber-reinforced polymer composites for automotive interior trim applications," *Journal of Materials Science* 49(6), 2630-2639. DOI: 10.1007/s10853-013-7965-6.
- Fortunati, E., Armentano, I., Zhou, Q., Puglia, D., Terenzi, A., Berglund, L. A., and Kenny, J. (2012). "Microstructure and nonisothermal cold crystallization of PLA composites based on silver nanoparticles and nanocrystalline cellulose," *Polymer Degradation & Stability* 97(10), 2027-2036. DOI: 10.1016/j.polymdegradstab.2012.03.027
- Garlotta, D. (2001). "A literature review of poly (lactic acid)," *Journal of Polymers & the Environment* 9(2), 63-84. DOI: 10.1023/A:1020200822435
- Huda, M. S., Drzal, L. T., Mohanty, A. K., and Misra, M. (2008). "Effect of fiber surface-treatments on the properties of laminated biocomposites from poly(lactic acid) (PLA) and kenaf fibers," *Composites Science & Technology* 68(2), 424-432. DOI: 10.1016/j.compscitech.2007.06.022
- Kang, J. T., and Kim, S. H. (2011). "Improvement in the mechanical properties of polylactide and bamboo fiber biocomposites by fiber surface modification," *Macromolecular Research* 19(8), 789-796. DOI: 10.1007/s13233-011-0807-y
- Kim, H. S., Park, B. H., Choi, J. H., and Yoon, J. S. (2008). "Mechanical properties and thermal stability of poly (L-lactide)/calcium carbonate composites," *Journal of Applied Polymer Science* 109(5), 3087-3092. DOI: 10.1002/app.28229
- Kumar, K. P., and Sekaran, A. S. J. (2014). "Some natural fibers used in polymer composites and their extraction processes: A review," *Journal of Reinforced Plastics & Composites* 33(20), 1879-1892. DOI: 10.1177/0731684414548612
- Lunt, J. (1998). "Large-scale production, properties and commercial applications of polylactic acid polymers." *Polymer Degradation & Stability* 59(1-3), 145-152. DOI: 10.1016/S0141-3910(97)00148-1

- Mustapa, I. R., Robert, A. S. and Ing, K. (2013). "Poly(lactic acid)-hemp-nanosilica hybrid composites: Thermomechanical, thermal behavior and morphological properties," *International Journal of Advanced Science and Engineering Technology* 3(1), 192-199. DOI: 10.1515/secm-2013-0119
- Ng, T. S., Ching, Y. C., Awanis, N., Ishenny, N., and Rahman, M. R. (2014). "Effect of bleaching condition on thermal properties and UV-transmittance of PVA/cellulose biocomposites," *Materials Research Innovations* 18(S6), 400-404. DOI: 10.1179/1432891714Z.000000000986
- Nurfatimah, B., Ching, Y. C., Luqman, C. A., Chantara, T. R., and Nor, A. (2014). "Effect of methyl methacrylate grafted kenaf on mechanical properties of polyvinyl chloride/ethylene vinyl acetate composites," *Composites Part A* 63, 45-50. DOI: 10.1016/j.compositesa.2014.03.023
- Nurfatimah, B., Ching, Y. C., Luqman, C. A., Chantara, T. R., and Nor, A. (2015). "Thermal and dynamic mechanical properties of grafted kenaf filled poly(vinyl chloride)/ethylene vinyl acetate composites," *Materials and Design* 65, 204-211. DOI: 10.1016/j.matdes.2014.09.027
- Oksman, K., Skrifvars, M., and Selin, J.-F. (2003). "Natural fibres as reinforcement in polylactic acid (PLA) composites," *Composites Science and Technology* 63(9), 1317-1324. DOI: 10.1016/S0266-3538(03)00103-9
- Petersson, L., and Oksman, K. (2006). "Biopolymer based nanocomposites: Comparing layered silicates and microcrystalline cellulose as nanoreinforcement," *Composites Science & Technology* 66(13), 2187-2196. DOI: 10.1016/j.compscitech.2005.12.010
- Qu, P., Tang, H., Gao, Y., Zhang, L., and Wang, S. (2010). "Polyethersulfone composite membrane blended with cellulose fibrils," *BioResources* 5(4), 2323-2336. DOI: 10.15376/biores.5.4.2323-2336
- Ray, S. S., and Okamoto, M. (2003). "Polymer/layered silicate nanocomposites: A review from preparation to processing," *Progress in Polymer Science* 28(11), 1539-1641. DOI: 10.1016/j.progpolymsci.2003.08.002
- Rayung, M., Ibrahim, N. A., Zainuddin, N., Saad, W. Z., Razak, N. I. A., and Chieng, B. W. (2014). "The effect of fiber bleaching treatment on the properties of poly (lactic acid)/oil palm empty fruit bunch fiber composites," *International Journal of Molecular Sciences* 15(8), 14728-14742. DOI: 10.3390/ijms150814728
- Rhim, J. W., Mohanty, A. K., Singh, S. P., and Ng, P. K. (2006). "Effect of the processing methods on the performance of polylactide films: Thermocompression versus solvent casting," *Journal of Applied Polymer Science* 101(6), 3736-3742. DOI: 10.1002/app.23403
- Rhim, J.-W., Hong, S.-I., and Ha, C.-S. (2009). "Tensile, water vapor barrier and antimicrobial properties of PLA/nanoclay composite films," *LWT-Food Science & Technology* 42(2), 612-617. DOI: 10.1016/j.lwt.2008.02.015
- Saba, N., Paridah, M. T., and Jawaid, M. (2014) "A review on potentiality of nano filler/natural fiber filled polymer hybrid composites," *Polymers* 6, 2247-2273. DOI:10.3390/polym6082247
- Shi, Q. F., Mou, H. Y., Gao, L., Yang, J., and Guo, W. H. (2010). "Double melting behaviour of bamboo fiber-talc-poly(lactic acid) Composites," *J. Polym. Environ* 18, 567-575.
- Shi, X., Duan, J., Lu, J., Liu, M., and Shi, L. (2014). "A novel fabrication method of network-like polyimide/silica composite microspheres with a high SiO<sub>2</sub> content," *Materials Letters* 128, 5-8. DOI: 10.1016/j.matlet.2014.04.049

- Siyamak, S., Ibrahim, N. A., Abdolmohammadi, S., Yunus, W. M. Z. B. W., and Rahman, M. Z. A. (2012). "Enhancement of mechanical and thermal properties of oil palm empty fruit bunch fiber poly (butylene adipate-co-terephthalate) biocomposites by matrix esterification using succinic anhydride," *Molecules* 17(2), 1969-1991. DOI: 10.3390/molecules17021969
- Tahan, L., Mehrali, S., Mottahedin, M., Fereidoon, L., and Metselaar, H. S. C. (2013). "Investigation of interfacial damping nanotube-based composite," *Composites Part B: Engineering* 50, 354-361
- Tan, B. K., Ching, Y. C., Gan, S. N, and Shaifulazuar, R. (2015). "Biodegradable mulches based on poly(vinyl alcohol), kenaf fiber, and urea," *BioResources* 10(3), 5532-5543. DOI:10.15376/biores.10.3.5523-5543
- Khoon, K. T., Ching, Y. C., Poh, S. C., Luqman, C. A., and Gan, S. N. (2015). "A review of natural fiber reinforced poly(vinyl alcohol) based composites: Application and opportunity," *Polymers* 7(11), 2205-2222. DOI:10.3390/polym7111509
- Vaibhav, V., Vijayalakshmi, U., and Roopan, S. M. (2015). "Agricultural waste as a source for the production of silica nanoparticles," *Spectrochimica Acta Part A: Molecular & Biomolecular Spectroscopy* 139, 515-520. DOI: 10.1016/j.saa.2014.12.083
- Valdés, A., Mellinas, A. C., Ramos, M., Garrigós, M. C., and Jiménez, A. (2014). "Natural additives and agricultural wastes in biopolymer formulations for food packaging," *Frontiers in Chemistry* 2, 6. DOI: 10.3389/fchem.2014.00006
- Wang, M., Wang, Z., Li, N., Liao, J., Zhao, S., Wang, J., and Wang, S. (2015). "Relationship between polymer–filler interfaces in separation layers and gas transport properties of mixed matrix composite membranes," *Journal of Membrane Science* 495, 252-268. DOI: 10.1016/j.memsci.2015.08.019
- Wu, C. S., and Liao, H. T. (2008). "Modification of biodegradable polylactide by silica and wood flour through a sol–gel process," *Journal of Applied Polymer Science* 109(4), 2128-2138. DOI: 10.1002/app.27988
- Yan, S., Yin, J., Yang, J., and Chen, X. (2007a). "Structural characteristics and thermal properties of plasticized poly (L-lactide)-silica nanocomposites synthesized by sol–gel method," *Materials Letters* 61(13), 2683-2686. DOI: 10.1016/j.matlet.2006.10.023
- Yan, S., Yin, J., Yang, Y., Dai, Z., Ma, J., and Chen, X. (2007b). "Surface-grafted silica linked with l-lactic acid oligomer: A novel nanofiller to improve the performance of biodegradable poly (l-lactide)," *Polymer* 48(6),1688-1694. DOI: 10.1016/j.polymer.2007.01.037
- Yang, H.-S., Kim, H.-J., Park, H.-J., Lee, B.-J., and Hwang, T.-S. (2007). "Effect of compatibilizing agents on rice-husk flour reinforced polypropylene composites," *Composite Structures* 77(1), 45-55. DOI: 10.1016/j.compstruct.2005.06.005
- Yong, K. C., Ching, Y. C., Mohamad, A., Lim, Z. K., and Chong, K. E. (2015). "Mechanical and thermal properties of chemical treated oil palm empty fruit bunches fiber reinforced polyvinyl alcohol composite," *J. Biobased Mater. Bioenergy* 9, 231-235.
- Yu, L., Dean, K., and Li, L. (2006). "Polymer blends and composites from renewable resources," *Progress in Polymer Science* 31(6), 576-602. DOI: 10.1016/j.progpolymsci.2006.03.002

- Yu, T., Ren, J., Li, S., Yuan, H., and Li, Y. (2010). "Effect of fiber surface-treatments on the properties of poly (lactic acid)/ramie composites," *Composites Part A: Applied Science & Manufacturing* 41(4), 499-505. DOI: 10.1016/j.compositesa.2009.12.006
- Zeng, Q., Yu, A., Lu, G., and Paul, D. (2005). "Clay-based polymer nanocomposites: Research and commercial development," *Journal of Nanoscience & Nanotechnology* 5(10), 1574-1592. DOI: 10.1166/jnn.2005.411
- Zhang, J., Lou, J., Ilias, S., Krishnamachari, P., and Yan, J. (2008). "Thermal properties of poly (lactic acid) fumed silica nanocomposites: Experiments and molecular dynamics simulations," *Polymer* 49(9), 2381-2386. DOI: 10.1016/j.polymer.2008.02.048

Article submitted: July 26, 2015; Peer review completed: September 13, 2015; Revised version received and accepted: November 2, 2015; Published: January 20, 2016.  
DOI: 10.15376/biores.11.1.2269-2286